Available online at www.sciencedirect.com
SCIENCE DIRECT®
Earth and Planetary Science Letters 243 (2006) 536–551
EPSL
www.elsevier.com/locate/epsl

Methodology of Curie discontinuity map development for regions with low thermal characteristics: An example from Israel

Lev V. Eppelbaum [a,*], Arkady N. Pilchin [b]

[a] Department of Geophysics and Planetary Sciences, Raymond and Beverly Sackler Faculty of Exact Sciences, Tel Aviv University, Ramat Aviv 69978, Tel Aviv, Israel
[b] Universal Geoscience and Environment Consulting Company, 205 Hilda Ave., Willowdale, Ontario, Canada M2M 4B1

Received 25 July 2005; received in revised form 21 December 2005; accepted 5 January 2006
Available online 3 March 2006
Editor: E. Boyle

Abstract

Analysis of available data indicates that different values of the Curie temperature for magnetite and titanomagnetites along with transition between ferric (Fe III) and ferrous (Fe II) iron could lead to significant errors in the Curie point depth determination using magnetic data. Based on analysis of geothermal and magnetic methods used for the Curie point depth determination in different regions it is shown that for conditions in the Eastern Mediterranean examination of the magnetic field should be used for determination of the bottom edges of magnetized bodies/layers only. The authors demonstrated that the depth of the bottom edges of magnetized bodies couldn't be greater than the depth of the Curie point for magnetite. On example of Israel and adjoining regions of the Eastern Mediterranean it is shown that in regions with a low heat flow and low vertical geothermal gradient, the depth of the Curie point is usually greater than that of the Moho discontinuity. An improved geothermal method of temperature calculation and other geothermal parameters analysis was used to determine the Curie point depth in the regions of the Eastern Mediterranean and adjoining areas. A new map of the Moho discontinuity for the region covering Israel, Jordan, Palestinian autonomy, Syria, Lebanon, and the eastern part of the Mediterranean Sea was composed. The Moho discontinuity map was utilized for the development of a first map of the Curie point depth for Israel.

Keywords: Curie point depth; rock magnetism; Moho discontinuity; gravitational field; Israel

1. Introduction and short review of the problem

It is widely accepted that the main ferromagnetic mineral in the lithosphere is magnetite (Fe_3O_4), with the Curie point of about 848–851 K [1,2]. Two main iron oxides: ferrous oxide (FeO, or wüstite) and hematite (α-Fe_2O_3) are paramagnetics, and maghemite (γ-Fe_2O_3) is the only iron oxide with ferromagnetic properties, having a Curie point of about 948 K. In natural occurrences, maghemite is predominantly formed by the low-temperature oxidation of magnetite; however, it is thermodynamically metastable and it converts to hematite when heated above ~523 K [3]. On the other hand, iron oxides are usually presented in compounds with some other minerals containing Ti, Mg, Ca, Ni, etc. For example, the main magnetic minerals of igneous rocks are titanomagnetites [1]. The Curie point of titanomagnetites is strongly depending on the amount

* Corresponding author. Fax: +972 3 6409282.
E-mail addresses: levap@post.tau.ac.il (L.V. Eppelbaum), apilchin1521@rogers.com (A.N. Pilchin).

0012-821X/$ - see front matter © 2006 Elsevier B.V. All rights reserved.
doi:10.1016/j.epsl.2006.01.003

and type of titanium and iron oxides in the compound rock or mineral [1,2,4,5], and their Curie point could vary from 373 to 823 K. Such low Curie point (373 K) is used in some cases to explain the shallow depths of the bottom edges of magnetic bodies (BEMB) occurring in ancient platforms [2].

Methods used for determination of the Curie point depth (CD) could be divided into two groups: (I) geothermal methods and (II) magnetic methods. Geothermal methods are based on utilization of such geothermal data as heat flow and/or vertical geothermal gradient, heat production and heat conduction. The difficulties in employing geothermal methods are always relating to the inability of taking direct measurements of geothermal parameters at great depths. At the same time, these methods have some advantages for determination of the CD, which are related to exact value of the Curie point and which should be specified as one of the initial conditions. The geothermal methods for the CD determination applied in some regions of geosynclines [6,7] and stable platforms [7,8] indicate that the CD could locate below the Moho discontinuity (MD). This fact is in agreement with the data of [9] showing that temperatures at MD of the Baltic shield and some other regions of Europe are significantly lower than that of magnetite's Curie point. Since practically all geothermal methods of temperature calculation depend on the position of the top and bottom surfaces of vital crust layers, it is clear that for regions with the CD depth greater than MD, knowledge of the MD position is crucial. The MD location in such regions is important not only for determination of exact thickness of the Earth's crust, but also because the heat production by the decay of radioactive elements is very small or absent below the MD [8,9]. Various authors examined different geothermal methods for the calculation of temperature at great depths [for instance, [8,10]]. Several results of CD determination using geothermal methods for some regions are presented in Table 1.

It should be stated that for the CD determination, it is not so much important which geothermal method is employed, but rather how to use that method. Incorrect use of any geothermal method will obviously lead to decrease in accuracy of CD determination, or even obtaining wrong results. Geothermal parameters obtained in regions of hot spring activity could not be used for such calculations. For example, use of geothermal methods for determination of the CD in some areas of Jordan [11,12] shows that the CD calculated value is even less than that of the BEMB defined using magnetic data analysis. In some other cases, investigators are utilizing typical average values of geothermal parameters for the continental shelf and oceanic crust to estimate the depth of the CD [13] instead of using real geothermal data observed in the region. It should be underlined that such estimations may cause significant errors.

Another geothermal method for temperature estimation is based on measurements of heat flow near the earth's surface, and these measured values assumed as unchanged with depth [10]. This method also cannot give accurate estimations of temperature, because it is a known fact that the geothermal gradient decreases with depth increase [[8], see also Appendix A]. On the other hand, determination of CD in such thermally active region as Armenia (with near-surface geothermal gradients of about 30 to 100 K/km) gave CD values between 6 and 12 km [14]. At the same time, a wide range of heat flow values was measured in this region (from 38 to 157 mW/m^2) [14,15]. The unstable geothermal regime of Armenia, with its obvious visible signs of the Quaternary volcanic activity, makes it extremely difficult to use geothermal methods for determining the CD in that region.

Table 1
Results of Curie point depth determination for some regions using geothermal data

Region	Heat flow (mW/m^2)	Geothermal gradient (K/km)	Curie point depth (km)	Reference
Basin and Range province, W. USA*	35–105	25–45	22	[85]
Eastern USA*	35–63	15–25	37	[85]
Middle-Kura depression, Azerbaijan (western part)	45–104	30–43	18–32	[6]
Middle-Kura depression, Azerbaijan (eastern part)	33–50	20–30	32–42	[6,8]
Lower-Kura depression, Azerbaijan	17–42	10–25	32–42	[6,8]
South-Caspian depression, Azerbaijan	17–42	10–20	44–50	♦
Jordan	16–123	11–94	10–35	[11]
Armenia	38–157	30–100	6–12	[14]

*The values of the heat flow and geothermal gradients for these regions are taken from [86].
♦Data computed by the authors of the paper.

The idea of using magnetic methods for determination of the Curie isotherm's depth is based on the theory proposed by Bhattacharyya [16] and elaborated further in [17] and [18]. In this method, the spectrum analysis of magnetic data is applied [17,18]. The employment of magnetic methods for CD localization utilizes the idea that since magnetic minerals are losing their magnetic properties below the CD, the depth of BEMB in an area should represent its CD. The term "magnetic crust" is interpreted as the position of the Curie point isotherm [4]. This idea gives the opportunity to use more commonly and relatively easily measured magnetic data for the CD estimations [4,18–20]. Results of the CD determination for some regions obtained using magnetic methods are presented in Table 2. Application of these methods is also based on the idea that defined depths of the Curie point could be used for the prognosis of temperature.

However, use of magnetic methods arises some problems, because it is unclear which value should be accepted as the Curie point. Should it be the Curie point of magnetite, or that of titanomagnetite? If it is the Curie point of titanomagnetite, which value between 373 and 823 K is the best match for a region under study without any knowledge about the concentration of Ti-oxides at different depths? On the other hand, magnetic methods are the only methods for determination of the BEMB depth and it is unknown how to convert those parameters to real temperature values within the crust and upper mantle. It is obvious that in different regions, the mineral concentration could also be different. This means that the CD determined for different regions will relate to different Curie points and those values could not be compared. Moreover, in some regions, the Ti-oxide concentration may be very low, as that in the Kura depression of Azerbaijan [6,8]. Such low values of Ti-oxide concentrations cannot also represent their regional values, and they could be only local. On the other hand, the BEMB values in regions of ancient platforms usually do not exceed 10–15 km [2,7], even though the Curie temperature depth of magnetite in such regions (calculated using geothermal data) is located at the depths of 40–50 km and more [7,8]. In many cases, the shallow depths of BEMB could be explained by ferric iron (Fe III) instability under high *PT* conditions with its transformation to ferrous iron (Fe II) [1,6,7,21]. Such a transition is usually taking place at temperature of about 843 K, but this temperature could be significantly reduced with increase of pressure [6,7,22]. The statement that pressure increases with depth is obvious. Under real conditions within the Earth's crust the transfer of ferric iron into ferrous takes place at the temperatures between 473 and 673 K [6,7]. It was also shown [6,7] that the position of BEMB best corresponds to depths of this temperature interval. All the data are in agreement with the known facts that not only magnetite and hematite [1,2], but also ferric iron-containing rocks and minerals are of secondary origin [23]. These facts illustrate that in many cases the position of the BEMB may be caused by ferric iron instability under high *PT* conditions, and not by the Curie point.

Table 2
The Curie point depth determined for some regions using magnetic methods

Region	Curie isotherm calculated using methods of magnetic data interpretation (km)	Reference
NW Ontario, Canada	9–16	[87]
Yellowstone National Park, USA	4–22	[18]
Yellowstone National Park, USA	7–17	[88]
Arizona, USA	2–30	[4]
Quseir, Egypt	10	[89]
Kyushu, Japan	6.5–15	[90]
Nevada, USA	5–30	[91]
Cascade Range, USA	9–15	[92]
S and S-E Asia	9–46	[20]
Volcanic area	4–22	[20]
Island arc	13–25	[20]
Back-arc rift	14–26	[20]
Marginal sea	12–30	[20]
Continent	9–45	[20]
Trench	30–45	[20]

Analysis of available data indicates [7] that the Curie isotherm should be used only for the determination of the maximum possible depths of BEMB. In such cases, for the calculation of the BEMB position, the Curie temperature of magnetite (848–851 K) should be used. A selection of the Curie temperature of magnetite is based on the following facts:

(1) magnetite and its compounds are characterized by the highest magnetic properties and magnetite is the most often encountered magnetic mineral in the Earth's crust,
(2) the Curie point of magnetite is the highest among the Curie points of commonly abundant magnetic minerals (it was noted above that maghemite is unstable above 523 K).

This means that the Curie isotherm, defined as the depth of the Curie point of magnetite for concrete area,

should have an equal depth or be deeper than any depth of the BEMB. For example, analysis of the CD and depth of BEMB for the Kura depression in Azerbaijan shows that only in 3 cases out of 17 those depths are equal, but in 14 other cases the CD is significantly greater than that of the BEMB [6,7]. This fact proves that the depth of Curie point for magnetite is the maximal possible depth for minerals to hold their magnetic properties.

From this point of view, it is unacceptable to use the depth of the BEMB instead of CD. Earlier [6,7] it was also proposed to use the depths of 473 and 673 K isotherms, along with the CD for analysis of the conditions for preservation of magnetic properties within the lithosphere. These isotherms could be used as limits of the temperature interval for the ferric–ferrous iron transition.

For determination of the BEMB location in Israel and adjoining areas of the Eastern Mediterranean, both quantitative methods of magnetic anomalies interpretation and 3-D combined modeling of magnetic and gravity fields [24] were successfully applied. For CD determination, geothermal methods described in [8], as well as another procedures [25,26], were realized. Simplified description of geothermal methods used for the analysis of geothermal regime and the CD determination in the regions under study is presented in Appendix A. It represents a standard layered model with some specifics of analysis and calculation of different geothermal parameters by use of boundary conditions between layers. An additional specific of using layered model in Israel consists of that the Curie point in this region is located deeper than the MD. This fact demands addition to the layered model at least one more layer below the MD, as well as some assumptions about the geothermal gradient change below the MD. This problem is directly associated with the known data that below the MD concentration of radioactive elements is substantially reduced and it should significantly reduce a role of radioactive decay on the value of geothermal gradient. On the other hand, in Israel significant volcanic and geodynamic activity was not observed. Considering these facts together with extremely low geothermal characteristics of the Earth's crust in Israel and surrounding areas and continuing cooling this crust from at least Cretaceous, we can assume that geothermal gradient right below the MD should not change significantly. From the abovementioned follows that for thermal calculations within a layer located right below the MD, value of geothermal gradient could be accepted as a constant.

2. Main geothermal features of Israel and adjacent areas

For the analysis of the geothermal regime of Israel and surrounding regions, geothermal data and results of previous geothermal analyses [7,10,27–37] were utilized. Regions of the Eastern Mediterranean (east of Crete) are represented by very low values of heat flow varying from 11 to 44 mW/m^2, with its average value of 30.8 mW/m^2 [10,37]. Those values are significantly lower than that of both the continental and the oceanic crust. The heat flow in the Dead Sea Basin, excluding the hot springs, varies in range of 35–40 mW/m^2 [28]. The heat flow for Israel varies from 7–20 to 80–93 mW/m^2, and in a few cases even higher, with an average regional value of less than 40 mW/m^2. The average heat flow for the Levantine part of the Arabian–Nubian shield is about 33–36 mW/m^2. Although Israel's territory is characterized by a low geothermal regime, hot springs in some areas (Sea of Galilee and Dead Sea [36]) produce a high (up to 100 mW/m^2 and higher) heat flow, but their influence is very local.

One of the most important problems of geothermics is the evaluation of heat sources and their distribution. It is widely accepted [for instance, [25,38]] that the main source of heat in the Earth's strata is the radioactivity of long-living radioactive elements such as U-235, U-238, Th-232, and K-40.

It is also known that in a homogeneous layer with heat production caused by radioactivity, the geothermal gradient is decreasing with depth increase (see Appendix A). Some results of analysis of geothermal gradients decreasing with a depth in different regions are presented in Table 3. This table shows calculated values of vertical geothermal gradient for regions with low heat flow (Israel), normal heat flow (Williston Basin of Canada, Middle-Kura depression of Azerbaijan, Central Ventura Basin of the USA), high heat flow (Krasnodar and Stavropol regions of Russia, Utah state of the USA), and some regions with very high heat flow (Salton Sea of the USA). These data support the fact of geothermal gradient decrease with a depth in regions with different geothermal regime. More detailed results of geothermal gradient change are presented in Table 3 for some areas of the Caucasus, because it is one of regions highly covered by geothermal investigations (it includes hundreds of temperature measurements at depths greater than 4, 5 and even 6 km, and thousands of temperature measurements at depths greater than 2 and 3 km). Moreover, geothermal data in this region were particularly analyzed for change of geothermal gradient with depth and in horizontal direction. The fact of significant

Table 3
Change of vertical geothermal gradient with depth for some regions

Region	Depth interval (m)	Average geothermal gradient (K/km)	Percentage of geothermal gradient near-surface (%)	Reference
Krasnodar region, Russia	0–2000	30–40	70	[8,15]
	2000–4000	30–35	65	[8,15]
	4000–6000	25–32	57	[8,15]
Stavropol region, Russia	0–2000	35–50	71	[8,15]
	2000–4000	35–45	67	[8,15]
	4000–6000	30–35	54	[8,15]
Middle-Kura depression, Azerbaijan	0–2000	25–43	76	[8,15]
	2000–4000	20–35	61	[8,15]
	4000–6000	20–30	42	[8,15]
Northern Israel	2300	18–20	46–54	[35]
Dead Sea region, Israel	2350–2750	16–22	20–61	[35]
Utah, USA	440–619	48	83	[93]
Salton Sea, USA	762–884	178.9	73	[94]
Central Ventura Basin, USA	1900–3600	23–27	70–86	[95]
Williston Basin, Canada	2000–3000	10–20	30–80	[96]
Michigan Basin, USA	Phanerozoic	17.5	41	[97]

decrease of geothermal gradient with depth, especially in near surface layers (first hundreds of meters and up to 1–2 km) shows that employing of geothermal gradients measured at shallow depths and accepted as unchanged with the depth for calculation of temperature at great depths can cause significant errors. This means that geothermal parameters measured near the Earth's surface should be used very carefully for temperature calculation. Taking into account all abovementioned, we applied for calculation of temperature mostly geothermal gradients calculated using temperature measurements at highest possible depth in each area. Simplified methods of geothermal data analysis and temperature calculations used for calculations of CD are presented in Appendix A.

3. Computing the Moho discontinuity depth in the Eastern Mediterranean

CD determination in the regions with low geothermal characteristics (heat flow and vertical geothermal gradient) is strongly dependent on the position of the Moho discontinuity (MD). During the last few decades, many values of MD were determined for Israel and the Eastern Mediterranean [11,12,37,39–45], but a very few attempts were realized to compose a map of the MD. Results of these determinations are presented in Table 4. These data indicate that values of the MD calculated by various investigators are in a satisfactory agreement.

The correlation method applied by the authors in [43] consisted of comparison of Moho depth obtained by deep seismic sounding (MD_{seism}) with the Bouguer gravity observed along the same seismic sections. Computed corresponding relationships between MD_{seism} and Bouguer gravity intensity was used as a basis for computing of a map of MD for all territory of Israel.

However, performed analysis of Bouguer gravity data together with the MD depth shows that the previously applied methods of its determination [43,44] need some corrections. The correlation between the Bouguer gravity ($\Delta g_{Bouguer}$) (main part of these data used are presented in Fig. 1) and values of MD for the Eastern Mediterranean points at presence of at least two independent data sets (Fig. 2). A graph in Fig. 2 was composed using analysis of $\Delta g_{Bouguer}$ from the Eastern Mediterranean Sea (including Cyprus and Erathosthenes seamount blocks). This figure testifies a sharp change in

Table 4
Comparison of results of Moho surface depth determination for some areas of the region under study (values are given in km)

Northern Israel	Central Israel	Southern Israel	Eastern Mediterranean Sea	Reference
–	26–30	18–42 30–35	18–24	[39]*
–	30–35	28–36	–	[40]**
–	–	36–40	23–27	[41]**
19–25	25–30	–	22	[42]**
–	25–30	30–42	22–25	[52]**
19–31	23–42	25–36	19–28	[43]*
23–25	24–28	32–40	20–24	[44]*
24–32	25–32		22–28	♦

*Data from the map of Moho discontinuity.
**Data from the profiles and single Moho depth determinations.
♦Data computed by the authors of the paper.

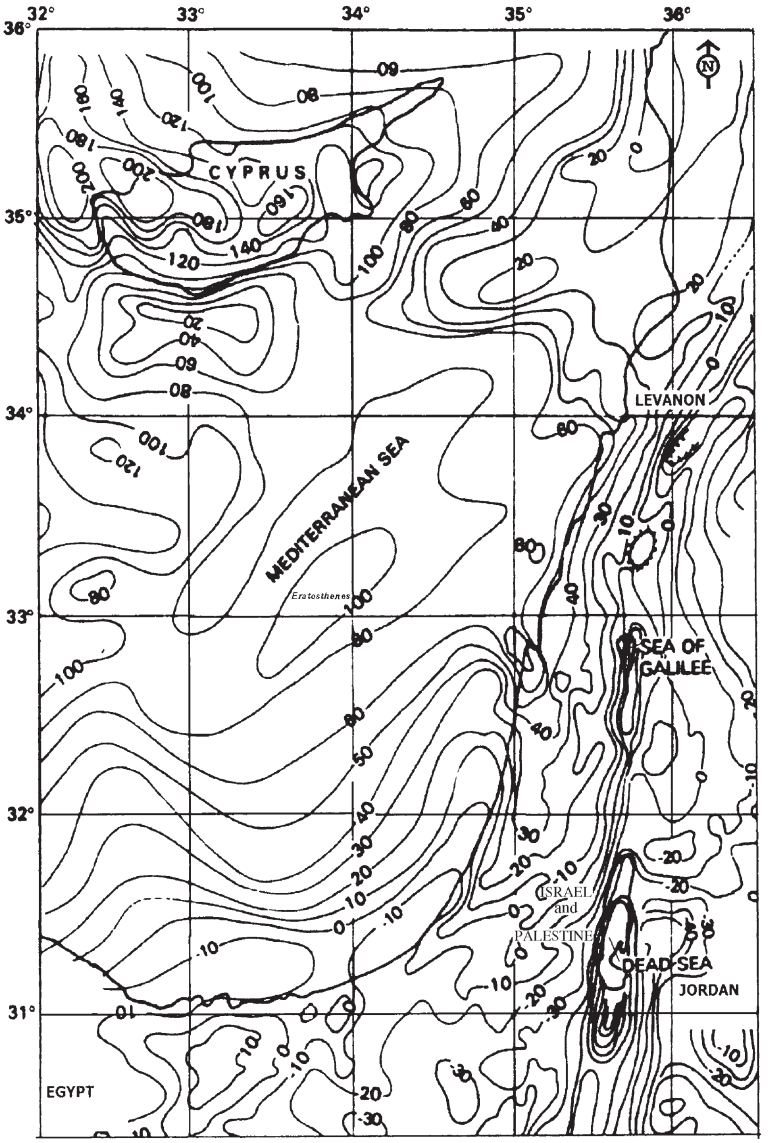

Fig. 1. Gravity map ($\Delta g_{\text{Bouguer}}$) of the studied region (after [42]).

the relationship between the MD (in km) and $\Delta g_{\text{Bouguer}}$ (in mGal s (10^{-5} m/s^2)) for these regions with the $\Delta g_{\text{Bouguer}}$ values below and above 80 mGal. Almost all values of $\Delta g_{\text{Bouguer}} > 80$ mGal belong to the Eratosthenes seamount and Cyprus block. Based on these relationships, the region under study was divided into a few sub-regions for more accurate determination of the MD position. These sub-regions are as follows: Israel, Eastern Mediterranean Sea without the Eratosthenes and Cyprus blocks, the Eratosthenes seamount, Cyprus block, Jordan, Syria and Lebanon. For analysis of this correlation between the $\Delta g_{\text{Bouguer}}$ and the MD depth beside [43,44], the data of [11,12,45–60] were also utilized. These data were analysed using methods described in [43,44]. Performed examination of the correlation between the MD and the $\Delta g_{\text{Bouguer}}$ indicates that in all cases a linear approximation could be assumed. Obtained equations of these approximations are presented in Table 5.

Based on the obtained equations (Table 5), for each mentioned sub-region a map of the MD has been created. After that, a common map of the MD representing all sub-regions under study was compiled. The final map of the MD for the studied region is presented in Fig. 3. This map covers Israel, Jordan, Palestinian autonomy, Syria, Lebanon, and the eastern part of the Mediterranean Sea. It is a first Moho discontinuity map joining all these areas to one unified map.

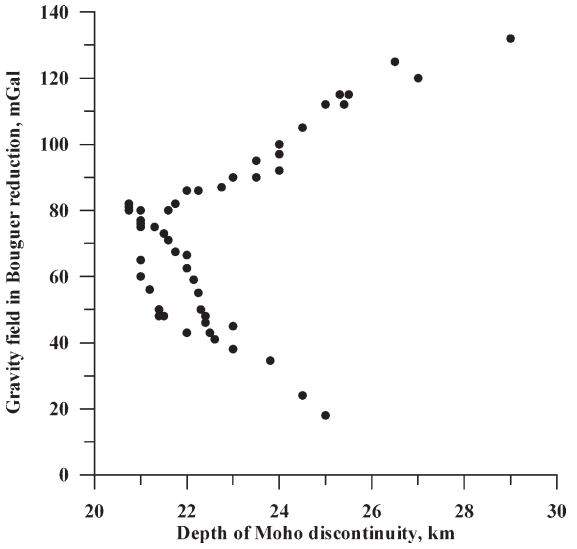

Fig. 2. Correlation between the gravity field in Bouguer reduction and Moho depth in the Eastern Mediterranean Sea (including Cyprus and Erathosthenes seamount blocks).

The obtained MD values were utilized for determination of the CD in Israel and some adjoining regions of the Eastern Mediterranean. In all cases of the CD determination, the Curie point of magnetite (851 K) was accepted as a general Curie point. The results of the CD calculations for Israel are presented in Fig. 5. Corresponding map of CD for other parts of the studied region has not been constructed because of lack of geothermal data in these areas. The CD estimations for the region of Easternmost Mediterranean Sea gave depths in the range of 38–50 km.

4. Computing of BEMB depths in Israel and Eastern Mediterranean

Computing of BEMB depths was performed using two ways: (1) 3-D combined magnetic-gravity modeling using GSFC (*Geological Space Field Calculation* [24]) program (significant part of the computed results is presented in [37]), and (2) advanced analysis of magnetic anomalies using their singular and characteristic points [24] (results of these investigations were partially reflected in [7]). In the first case a direct problem solution is realized and in the second—inverse problem solution. According to our experience, a first way is more exact and reliable since we apply combined analysis of two potential fields (magnetic and gravity) in many cases supported by seismic data utilization (in areas where seismic sections were constructed). At the same time practical realization of the first way demands time expenditures in a few tens of time exceeding the second way application. Some calculated BEMB depths for the Eastern Mediterranean Sea and Israel are presented in the map of the total magnetic field of the same region (Fig. 4).

5. Discussion and some geological and geophysical applications

The Bouguer gravity map of the Eastern Mediterranean (Fig. 1) shows that the main features of Bouguer gravity in the region are: (1) its values are maximal in Cyprus (+80–200 mGal) and the Eratosthenes seamount (+80–120 mGal), even though seismic data point at presence of continental crust in these areas [37,41] with significant increase of MD in regions of Eratosthenes (up to 31–32 km [37] and 26–29 km [41]) and Cyprus (up to 26–29 km [37] and 35 km [41]); (2) its values are positive in continental areas of western Syria, Lebanon, northern and central Israel (maximal values of Bouguer gravity in continental areas are about +70 mGal near Haifa, Israel), and some areas of southern Israel; (3) its values are negative in south easternmost part of the Eastern Mediterranean Sea (right offshore Egypt and Israel) and in the same areas they are positive right onshore. All these features could be clearly seen in Figs. 1 and 2, and it explains the fact of the Bouguer gravity increasing with increase of MD. These data show that those regions have very unusual composition, which could relate to specific tectonic evolution. It was previously shown [37,42] that density of crustal rocks in Israel is unusually high. Abnormal behavior of the Bouguer gravity in Cyprus and Eratosthenes seamount is obviously related to violation of isostatic equilibrium there. This hypothesis is supported by the fact of continuous uplifting in Cyprus area since Cenozoic. It also should be noted that values of the Bouguer gravity are also positive in continental part of eastern Syria (see for example Fig. 4 in [42], and Fig. 3 in [45]). Seismic cross sections used for compiling Fig. 1 and their locations are shown in [37,39–42,44,45,47,48].

Table 5
Equations for calculation of Moho discontinuity depth in different parts of the region using gravity field in the Bouguer reduction (depth of Moho discontinuity is in km and $\Delta g_{\text{Bouguer}}$ in mGal)

Region	Applied equation
Israel	$H_{\text{MD}} = 32.2 - 0.171 \cdot \Delta g_{\text{Bouguer}}$
South-Eastern Mediterranean	$H_{\text{MD}} = 26.08 - 0.0658 \cdot \Delta g_{\text{Bouguer}}$
Cyprus block	$H_{\text{MD}} = 22.0 + 0.175 \cdot (\Delta g_{\text{Bouguer}} - 80)$
Eratosthenes block	$H_{\text{MD}} = 22.04 + 0.124 \cdot (\Delta g_{\text{Bouguer}} - 80)$
Jordan	$H_{\text{MD}} = 31.35 - 0.0833 \cdot \Delta g_{\text{Bouguer}}$
Syria and Lebanon	$H_{\text{MD}} = 32.15 - 0.1026 \cdot \Delta g_{\text{Bouguer}}$

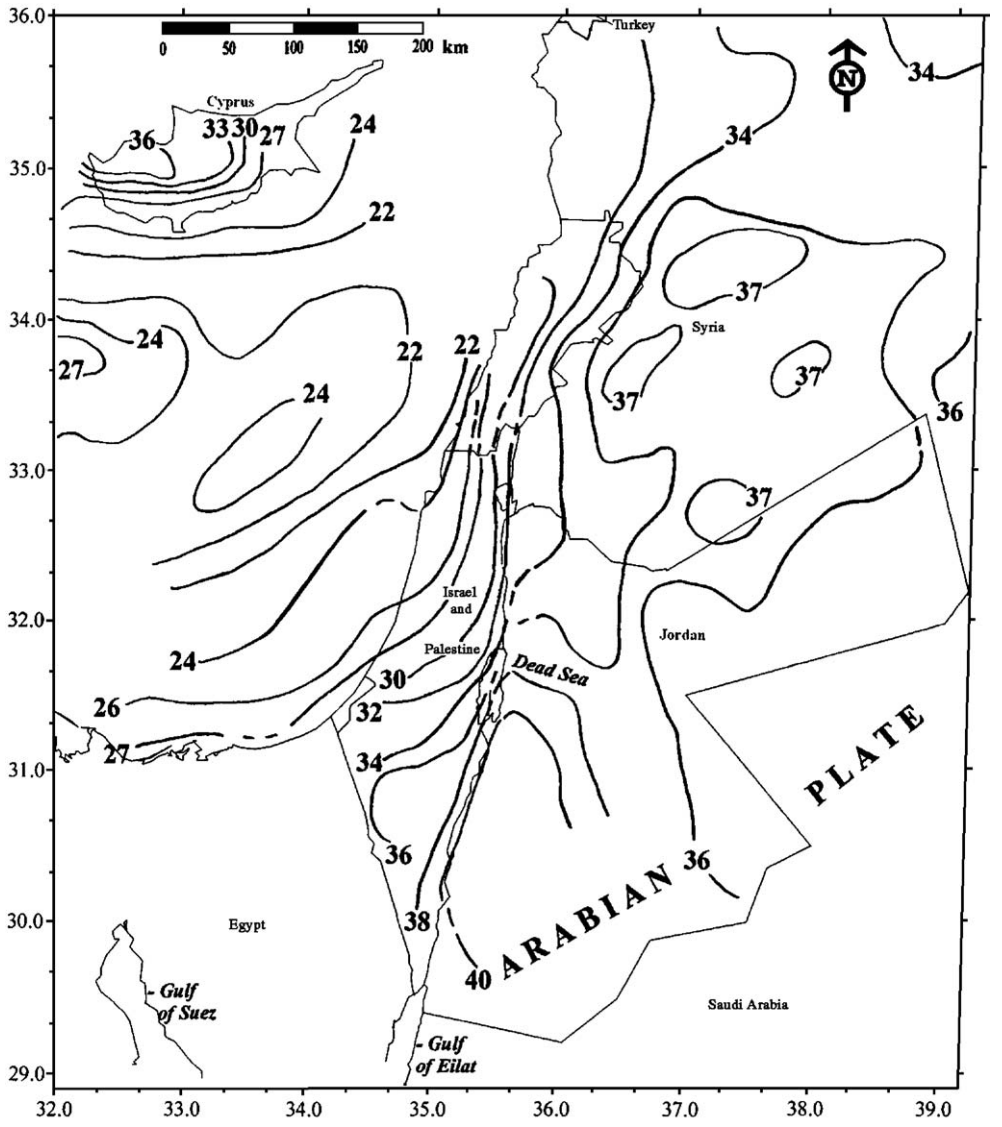

Fig. 3. Map of the Moho discontinuity depth for the Eastern Mediterranean Sea and adjoining continental areas (isolines are given in km).

A newly constructed map of the MD for the Eastern Mediterranean (Fig. 3) is in a good agreement with the previously published MD maps and MD estimations (see Table 4) and [11,12,45,58–60]. Analysis of the MD map (Fig. 3) indicates that thickness of the Earth's crust in Cyprus (26–36 km) is much greater than that of the oceanic crust. At the same time at the Cyprus region registered low heat flow values—significantly lower than that conventional values for oceanic crust. Analysis of the Bouguer gravity in Cyprus region shows that Earth's crust here cannot represent fragments of the ancient continental crust, because the continental crust of its regular thickness cannot produce such intensive gravity anomalies. Examination of the possible density of continental rocks necessary for the creation of such significant anomaly as that of western Cyprus shows that the density of those rocks should be higher than that of the regular continental crust. For the Cyprus region (as it may be seen in Figs. 1 and 2) we have an increase of the $\Delta g_{\text{Bouguer}}$ intensity with an increase of MD. This fact may signify that the Cyprus region is not a typical crustal structure. Indeed, density of the Earth's crust is notably lower than that of the upper mantle. This means that an increase in the thickness of the typical crust (MD increasing) should lead to decrease in the Bouguer gravity. However, for Cyprus, the $\Delta g_{\text{Bouguer}}$ values are increasing with MD increase. This fact testifies for anomalously high density distribution in this region. This could happen if the crust of western Cyprus is

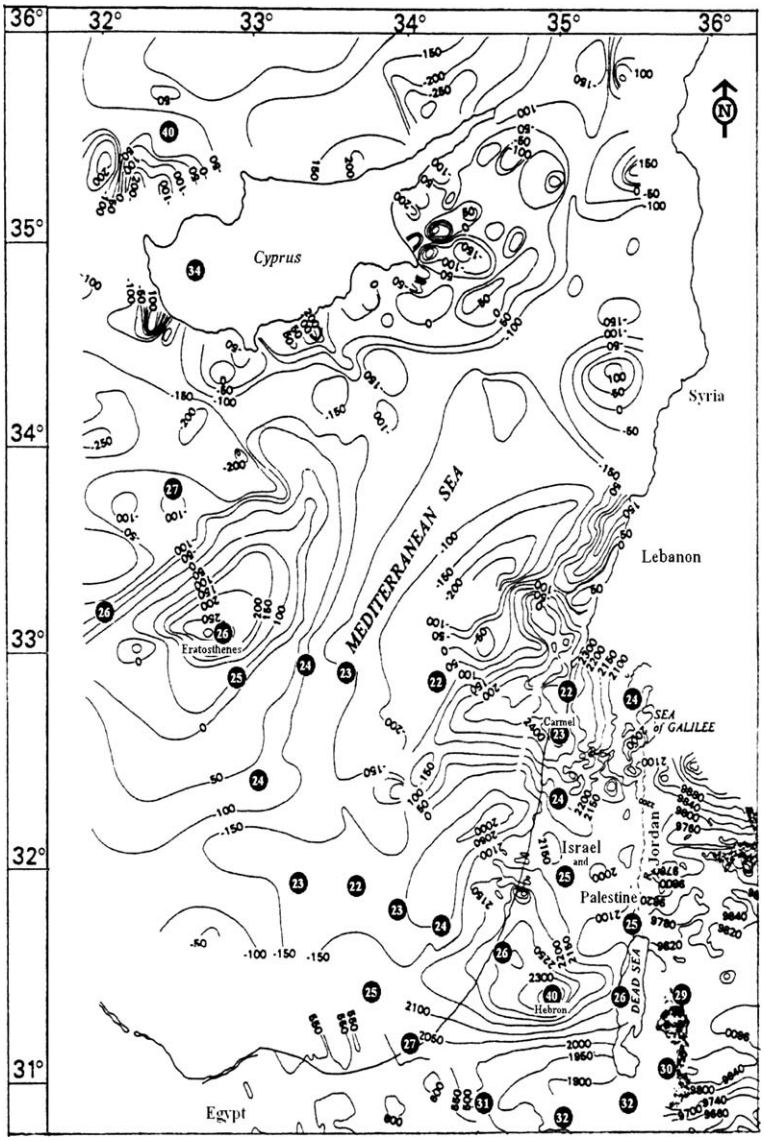

Fig. 4. Map of the total magnetic field of the studied region (modified after [37]). White values in black circles show calculated values of BEMB.

composed of a doubled ocean crust formed in ancient times by an obduction of the oceanic crust onto itself with its subsequent immersion and partial destruction. The mechanism of such an obduction with the following immersion of the composite block is described in [61]. This hypothesis is in accordance with the results of [62] showing that two distinct peridotite units were found within the Troodos massif in Cyprus.

Results of MD determination in the Eastern Mediterranean, and especially in the region under study, demonstrate that the MD in all cases is greater than 20 km. This fact may be explained that oceanic crust in these areas is rather transitional between oceanic and continental than oceanic.

Interestingly, the northern Israel is also characterized by unusually high density of crustal rocks [37,42]. This could relate to the presence of ancient oceanic crust fragments within the continental crust. Folkman and Bein [46] suggested that a deeply buried oceanic crust underlies the area north of the Hebron suture zone in central Israel. Seismic investigations indicate that along the southern part of Dead Sea fault zone and the Gulf of Eilat the lower crust is separated from the upper mantle by a 5-km-thick transition zone in which the velocity increases rapidly and smoothly from 6.7 km/s in the lower crust to 8 km/s in the upper mantle [40]. Some discontinuity was also found here, at the depth of 55 km within the upper mantle, below which the velocity

increases from 8.0 to 8.6 km/s [40]. These results point to the existence of two plates just under the crust, one of which may be a remnant of the Precambrian oceanic crust. This could also explain unusual values of Bouguer gravity in areas of South-Eastern Mediterranean where right off shore negative Bouguer gravity values were registered and its positive values onshore next to these areas (Fig. 1). This fact also wires the possibility that in the past oceanic lithosphere underthrust continental crust of southern Israel and adjoining areas of Egypt.

Buried peridotite plates were also found at different levels within the Earth's crust and upper mantle of some other regions [61]. Analysis of equations presented in Table 5 indicates that the most contrast change of the MD with change of the Bouguer gravity is related to Israel and Cyprus. This points to more complex crustal composition in Israel and Cyprus by comparison with other regions presented in Table 5.

Fascinatingly, obvious distribution of ophiolites in the Eastern Mediterranean is restricted to areas limited from the south by Crete–Cyprus–Baer-Bassit line [63]. At the same time, in the southern part of Eastern Mediterranean no obvious signs of presence of an ocean crust were observed. Since ophiolites, as it is widely believed, are remnants of the ocean crust [64], does it mean that ocean crust does not exist in the southern part of the Eastern Mediterranean? We propose that response must be a negative one. However, this fact could raise some questions about the age of the oceanic crust in the Eastern Mediterranean. Such crust could be significantly older than that of the Mesozoic age. There are also some indirect data which point to the presence of ocean crust fragments in the southern Eastern Mediterranean. Proterozoic ophiolites are well known along both sides of the Red Sea. In southern Israel, olivine rocks and serpentinites were found in Timna Igneous Complex, central Negev [65–67], Makhtesh Ramon area [68], and in dykes of Nahal Ardon [69]. In the Makhtesh Ramon area basalts containing 10–20% of olivine phenocrysts were described [66]. This could relate to the presence of a peridotite layer in the upper mantle of the region.

The main features of the CD as well as tectonic evolution of Israel, Eastern Mediterranean and adjoining regions are strongly related to very low geothermal regime in these regions (see above).

Results of paleogeothermal analysis [31] indicate that the warming of the upper crustal layers in the Judea Desert plateau (Israel) took place in the Mesozoic period and the geothermal gradient reached the maximum of 40 K/km in the Cretaceous. Then it decreased to 20 K/km from the Late Cretaceous to the Miocene. The cooling process is continuing to the present time [35]. Results of other investigations [34] also notify the cooling of the region since the Late Devonian–Early Carboniferous period. Temperature data observed in Atlit-1 borehole (northern Israel) shows the cooling from the geothermal gradient of 50 K/km in Mesozoic to ~18–20 K/km at present time [70]. Similar data from Ga'ash-2 and Devora-2A boreholes (northern Israel) also display a reduction of the geothermal gradient from the Mesozoic period [70]. In southern Israel, cooling took place from the Early Jurassic [71], and the present geothermal gradients are in the range of 19–20 K/km for the Early Jurassic rocks. The maximum of temperature was also defined for the Pozanti–Karsanti ophiolite, Turkey, at about 90–94 Ma ago (also Cretaceous) [72]. Another proof of low geothermal characteristics of the region is the discovery of diamonds in Makhtesh Ramon (southern Israel) [73] and Syria [74,75], since it is a well-known fact that diamonds were found exclusively in regions with a heat flow less than 40 mW/m^2 [76]. Such values of heat flow are among the lowest cratonic heat flows [77]. An extremely large number of serpentinite and ophiolite occurrences in the northeastern Mediterranean, Cyprus, Syria and Turkey [63] could be also assumed as a marker of low geothermal regime in the region. Some authors indicate the presence of serpentinites in the Precambrian of the Sinai Peninsula [49,63,78]. It was shown earlier that the serpentinization process could play a significant role in the tectonic processes of regions with a low temperature regime [61]. Such a low geothermal regime is the main reason of a very deep position of CD (38–46 km in some regions of Israel and 38–50 km in the Eastern Mediterranean) (Fig. 5). Interestingly, the great values of the CD (42–50 km) were obtained for some deep depressions of geosynclinal regions of Azerbaijan [6,7] (see also Table 1) and in ancient platforms (40–50 km and more) [7]. Our estimations of the CD gave depths of about 40–45 km in the ancient East-European platform, about 35–40 km in Western-Siberian region, and about 45–50 km for the Ural Mountains. At the same time, CD estimations for such ancient region as Brazil gave 30–37 km using geothermal data and 31 km for BEMB using magnetic methods [79]. A cold Earth's crustal region is also known in Germany [80,81], where some rocks of the Paleozoic magnetization have neither been in thermodynamic equilibrium nor under conditions of serpentinization (between 473 and 673 K) since the Paleozoic. There is evidence that in some other regions, rocks were never heated past the Curie point [82]. Samples of such rocks were found, for instance, in the Rand

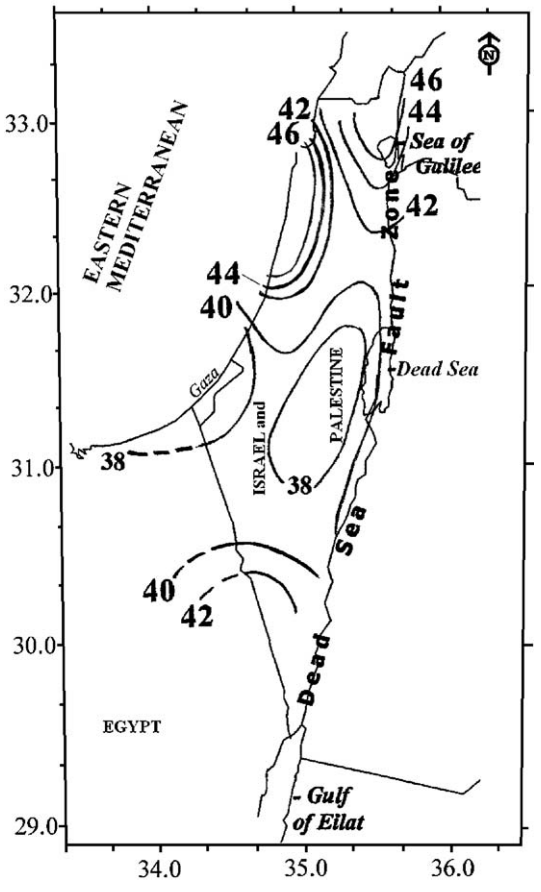

Fig. 5. Map of the Curie point depth for Israel (isolines are given in km).

Mountain schist and southern California [82]. Magnetic metamorphic minerals of these assemblages were equilibrated within the glaucophane–lawsonite (blueschist) field, and they had been buried for a long period at the great depths within the Earth, but they were never heated above the Curie temperatures of their ferromagnetic minerals [82]. In both abovementioned areas, rocks were buried to at least 20 km depth and held at temperatures below or about 573 K.

Fig. 5 illustrates that the CD in Israel is increasing to the north, where its value is about 42–46 km. CD relatively reduced to 38–40 km in central Israel and northern Negev, and it is again increasing to the south (up to 40–42 km and possibly more). Such a division of Israel is mostly controlled by its geothermal regime. The developed map correlates well with the results of previous geophysical and geological investigations. For example, minimal depths (38–40 km) of the CD correspond to the geological–geophysical structure known as a Hebron magnetic anomaly. A few authors [42,46,55,83] underline the importance of the Hebron magnetic anomaly area for understanding the structure of the Earth's crust in Israel. Eppelbaum et al. [84] based on CD and MD analysis and quantitative examination of magnetic anomaly suggested that the main source of this anomaly is a mantle diapir.

Ben-Avraham and Ginzburg [42] have shown that the territory of Israel could be divided into three huge terrains: Galilee–Lebanon, Judea–Samaria, and Negev. The position of these terrains has definite correlation with the determined location of the CD. The composed CD map is also in a good agreement with the results of paleogeothermal investigations in the region (see above) showing that present day cooling started in central Israel in the Cretaceous, and in southern Israel—between the Devonian and the Jurassic. This could be a reason of more cold crustal regions in southern Israel comparing to that of central Israel. There is no direct correlation between the position of the CD and the magnetic minimums and maximums, but position of lower depths of the CD indicates that in southern Israel there exists some increase in geothermal characteristics (heat flow and vertical geothermal gradient). Such an increase could relate to some increase in permeability of the lower crust and upper mantle, which could cause convectional heat and fluid transfer. Both fluid and heat transfers are significant for position of the CD and the BEMB. The heat transferred from the mantle will obviously increase the temperature and decrease CD. The fluid transfer will increase the oxidation regime and depth of ferric iron oxide stability, which leads to an increase of the BEMB depth. Comparison of both the CD and BEMB for regions of Israel illustrates that the CD in all cases is greater than the BEMB, and values of BEMB depths vary in interval of 20–35 km.

6. Conclusion

Analysis of geothermal and magnetic methods for determination of the Curie point depth in regions of the Eastern Mediterranean Sea and adjacent areas indicates that magnetic methods could be used only for the depth of the bottom edges of magnetized bodies determination, and those methods should not be used for the Curie point depth calculation.

A new map of the Moho discontinuity was composed for the region covering Israel, Jordan, Palestinian autonomy, Syria, Lebanon, and the eastern part of the Mediterranean Sea. This is the first Moho discontinuity map covering all these regions together.

Based on combined analyses of geothermal, tectonic, seismic, gravity, magnetic and other geological and

geophysical data, the first map of the Curie point depth in Israel was compiled.

Comparison of depths for both the Moho discontinuity and the Curie point in the region under study indicates that the Curie point depth is greater than that of the Moho discontinuity.

Acknowledgement

We thank Dr. T. Wonik and an anonymous reviewer for their useful comments and suggestions.

Appendix A. Applied method of geothermal analysis and temperature determination

Heat transfer in the Earth can be described using the heat conductivity equation [26]:

$$c\rho\left(\frac{\mathrm{d}T(z,t)}{\mathrm{d}t}\right)=\mathrm{d}\left(\frac{\lambda \mathrm{d}T(z,t)}{\mathrm{d}z}\right)\Big/\mathrm{d}z+\mathrm{d}\left(\frac{\lambda \mathrm{d}T(x,t)}{\mathrm{d}x}\right)\Big/\mathrm{d}x+\mathrm{d}\left(\frac{\lambda \mathrm{d}T(y,t)}{\mathrm{d}y}\right)\Big/\mathrm{d}y+H(x,y,z,t). \quad (A1)$$

Here $T(z, t)$, $T(x, t)$ and $T(y, t)$ are the temperatures, $H(x, y, z, t)$ is the heat production as a function of dimensions z, x, y and time t, c is the heat capacity, ρ is the density, and λ is the heat conduction of the rock composing the layer, depth z is increasing from the earth's surface downwards.

For applying Eq. (A1), we need to introduce some assumptions for the parameters of the equation [26,25]. Most of the Earth's crust layers (bodies) were formed millions of years ago and it can be assumed that for small periods of geological time, the distribution of temperature into those layers did not vary with time, and that their thermal regime was stable.

These assumptions and the fact that for the most stable regions, horizontal geothermal gradients ($\mathrm{d}T/\mathrm{d}x$, $\mathrm{d}T/\mathrm{d}y$) are much lower than the vertical geothermal gradient [8], let's present Eq. (A1) as:

$$\frac{\mathrm{d}Q}{\mathrm{d}z}+H(z)=0. \quad (A2)$$

Here Q is the heat flow

$$Q=\frac{\lambda \mathrm{d}T(z)}{\mathrm{d}z}, \quad (A3)$$

and $T(z)/\mathrm{d}z$ is the vertical geothermal gradient G.

Eq. (A2) can be thought of as an equation of heat conduction in an isotropic layer. Therefore we can write

$$\mathrm{d}\left(\frac{\lambda \mathrm{d}T(z)}{\mathrm{d}z}\right)/\mathrm{d}z+H(z)=0. \quad (A4)$$

For any arbitrary layer i, this heat conduction equation will be:

$$\mathrm{d}\left(\frac{\lambda_i(\mathrm{d}T_i(z))}{\mathrm{d}z}\right)/\mathrm{d}z+H_i=0. \quad (A5)$$

or

$$\mathrm{d}\left(\frac{\mathrm{d}T_i(z)/\mathrm{d}z}{\mathrm{d}z}\right)=-H_i/\lambda_i. \quad (A6)$$

Eq. (A6) may be written as:

$$\mathrm{d}(\mathrm{d}T_i(z)/\mathrm{d}z)=-(H_i/\lambda_i)\mathrm{d}z. \quad (A7)$$

Evaluation of a definite integral for Eq. (A7) with lower limit z_i and upper limit z_{i-1} gives:

$$(\mathrm{d}T_i(z)/\mathrm{d}z)_i=(\mathrm{d}T_i(z)/\mathrm{d}z)_{i-1}-(H_i/\lambda_i)(z_i-z_{i-1}). \quad (A8)$$

Here $(\mathrm{d}T_i(z)/\mathrm{d}z)_i$ and $(\mathrm{d}T_i(z)/\mathrm{d}z)_{i-1}$ are the values of the geothermal gradients in the layer i near surfaces z_i and z_{i-1}, respectively.

Since the values of the heat production H_i and interval thickness (z_i-z_{i-1}) are always positive, it is clear from Eq. (A8) that the geothermal gradient $\mathrm{d}T_i(z)/\mathrm{d}z$ decreases with depth increasing. Moreover, using the definition of the heat flow in Eq. (A3), Eq. (A8) may be transformed to the following type:

$$Q_i=Q_{i-1}-H_i(z_i-z_{i-1}). \quad (A9)$$

Here Q_i and Q_{i-1} are the heat flows at the depths z_i and z_{i-1}, respectively.

It is obvious from Eq. (A9) that the value of heat flow is also decreasing with depth. Eq. (A9) could also be obtained through the evaluation of a definite integral for Eq. (A2) with the lower limit z_i and upper limit z_{i-1}. Both Eqs. (A8) and (9) show that regardless of which geothermal method used for calculating temperatures, it should be taken into account that values of both the geothermal gradient and the heat flow are reducing with depth within the Earth's crust.

Evaluation of a definite integral for Eq. (A8) with the lower limit z_i and upper limit z_{i-1} gives:

$$T_i = T_i(z_{i-1}) + (\mathrm{d}T_i(z_i)/\mathrm{d}z)_{i-1}(z_i - z_{i-1}) - \frac{(H/\lambda_i)(z_i - z_{i-1})^2}{2}. \quad \text{(A10)}$$

Here $T_i(z_i)$ and $T_i(z_{i-1})$ are the values of the temperatures in the layer i nearby the surfaces z_i and z_{i-1}, respectively.

Eq. (A10) could be used for calculating temperature values within any layer and it already accounts for the geothermal gradient decrease within the layer.

In most cases, instead of using values H_i and λ_i, the value of their ratio H_i/λ_i could be used, because both Eqs. (A8) and (A10) contain this ratio [8]. This ratio may be simply defined for different regions just using the field measurements of temperatures at different depths [8] using equation

$$\frac{H_i}{\lambda_i} = \frac{G_{i-1} - G_i}{z_i - z_{i-1}}. \quad \text{(A11)}$$

Eq. (A10) could be used for calculation of temperature values within any layer and it already accounts for the geothermal gradient decrease within the layer.

Since Eqs. (A8) and (A10) were received for distribution of geothermal gradients and temperatures in an arbitrary layer of the earth strata, it is necessary to evaluate the distribution of those geothermal parameters with depth in all strata. For this purpose the initial conditions and boundary conditions for geothermal parameters on the surfaces separated one layer from another can be used [26]. Since values of temperature and heat flow are continuous values, they could be used for setting of initial and boundary conditions for an arbitrary at a certain time ($t=0$). The initial condition can be represented by function describing the initial temperature distribution in the layer or the package of layers.

It is obvious that the temperature on the surface separated one layer from another is the same for both contacting layers:

$$T_i(z_{i-1}) = T_{i-1}(z_i). \quad \text{(A12)}$$

The amount of heat flow leaving one layer exactly corresponds to the amount entering the layer occurring above the first one:

$$Q_i(z_{i-1}) = Q_{i-1}(z_{i-1}) \quad \text{(A13)}$$

or

$$\frac{\lambda_i \mathrm{d}T_i(z_{i-1})}{\mathrm{d}z} = \frac{\lambda_{i-1}\mathrm{d}T_{i-1}(z_{i-1})}{\mathrm{d}z} \quad \text{(A14)}$$

Eqs. (12)–(14) present the boundary conditions between any two consecutive layers and they can be used for determination of geothermal gradient and initial temperature for a lower layer knowing geothermal parameters for layer above it.

This method is described in detail in [8]. Based on detail analysis of heat production H_i and conductivity coefficient λ_i for rocks typical for middle and lower crust layers it was also shown [8] that the ratio H_i/λ_i is constant for a wide range of PT conditions. For Curie point depth (CD) calculation in Eq. (A10) the value of temperature on the left side was accepted as the value of the Curie point for magnetite. The value of the depth z on the right side of the Eq. (A10) was accepted as unknown variable and its value was calculated according to values of all other parameters of the equation.

References

[1] T. Nagata, Rock Magnetism, Maruzen, Tokyo, 1961.
[2] D.M. Pechersky, V.I. Bagin, S.Yu. Brodskaya, Z.V. Sharonov, Magnetism and Conditions of Igneous Rocks Generation, Nauka, Moscow, 1975 (in Russian).
[3] C.B. De Boer, M.J. Dekkers, Grain-size dependence of the rock magnetic properties for a natural maghemite, Geophys. Res. Lett. 23 (1996) 2815–2818.
[4] P.E. Byerly, R.H. Stolt, An attempt to define the Curie point isotherm in northern and central Arizona, Geophysics 42 (1977) 1394–1400.
[5] T. Nishitani, M. Kono, Curie temperature and lattice constant of oxidized titanomagnetite, Geophys. J. R. Astron. Soc. 74 (1983) 585–600.
[6] A.N. Pilchin, B.E. Khesin, On possible nature of the magnetoactive bodies bottom edges, Razved. Geofiz. 92 (1981) 123–127 (in Russian).
[7] A.N. Pilchin, L.V. Eppelbaum, Determination of the lower edges of magnetized bodies by using geothermal data, Geophys. J. Int. 128 (1997) 167–174.
[8] A.N. Pilchin, Geothermal regime of the earth crust of Kura Depression and its influence on the pressure distribution, Ph. D. Thesis (1983) Geoph. Inst. of the Georgian Academy of Sci. (in Russian).
[9] V. Čermák, L. Bodri, Three-dimensional deep temperature modeling along the European geotraverse, Tectonophysics 244 (1995) 1–11.
[10] E.V. Verzhbitsky, The Geothermal Regime and Seafloor Tectonics of Marine Basins along the Alpine–Himalayan Belt, Nauka, Moscow, 1996 (in Russian).
[11] A. Al-Zoubi, Deep geologic composition of Jordan by geophysical data, Ph.D. thesis, Mining Institute (1992), Sankt-Petersburg (in Russian).

[12] A. Al-Zoubi, Z. Ben-Avraham, Structure of the earth's crust in Jordan from potential field data, Tectonophysics 346 (2002) 45–59.
[13] C. Fichler, E. Rundhovde, O. Olesen, B.M. Sæther, H. Rueslåtten, E. Lundin, A.G. Dore, Regional tectonic interpretation of image enhanced gravity and magnetic data covering the mid-Norwegian shelf and adjacent mainland, Tectonophysics 306 (1999) 183–197.
[14] M. Badalyan, Geothermal features of Armenia: a country update, Trans. of the World Geothermal Congress (2000), Kyushu—Tohoku, Japan, May 28–June 10 2000, 2000, pp. 71–76.
[15] K.M. Kerimov, A.N. Pilchin, T.G. Gadzhiev, G.Y. Buachidze, Geothermal Map of the Caucasus, Scale 1:1,000,000 (1989) Baku, Cartographic Plant No. 11 (in Russian).
[16] B.K. Bhattacharyya, Continuous spectrum of the total magnetic field anomaly due to a rectangular prismatic body, Geophysics 31 (1966) 97–121.
[17] A. Spector, F.S. Grant, Statistical models for interpreting aeromagnetic data, Geophysics 35 (1970) 293–302.
[18] B.K. Bhattacharyya, L.K. Leu, Analysis of magnetic anomalies over Yellowstone National Park. Mapping the Curie-point isotherm surface for geothermal reconnaissance, J. Geophys. Res. 80 (1975) 461–465.
[19] Y. Okubo, T. Matsunaga, Curie-point depth in northeast Japan and its correlation with regional thermal structure and seismicity, J. Geophys. Res., Solid Earth 99 (B11) (1994) 22363–23371.
[20] A. Tanaka, Y. Okubo, O. Matsubayashi, Curie point depth based on spectrum analysis of the magnetic anomaly data in East and Southeast Asia, Tectonophysics 306 (1999) 461–470.
[21] D.M. Sherman, The nature of the pressure induced metallization of FeO and its implications to the core–mantle boundary, Geophys. Res. Lett. 16 (6) (1989) 515–518.
[22] V.A. Kurepin, Activity of components, thermodynamic characteristics of reactions and phase equilibrium in system Fe–O by high temperature and pressure, Geokhimiya 10 (1975) 1475–1483 (in Russian).
[23] M. Pilchin, A. Pilchin, Instability of some iron containing minerals under low temperature conditions, Trans. of 17th General Meet. of Intern. Mineral. Assoc., Toronto, 1998, p. A24.
[24] B.E. Khesin, V.V. Alexeyev, L.V. Eppelbaum, Interpretation of geophysical fields in complicated environments, Ser: Modern Approaches in Geophysics, Kluwer Acad. Publ., Dordrecht/Boston/London, 1996.
[25] O. Kappelmeyer, R. Haenel, Geothermics with special reference to application, Gebruder Borntrargen, Berlin–Stuttgart, 1974.
[26] H.S. Carslaw, J.C. Jaeger, Conduction of Heat in Solids, 2nd edition. Oxford Univ. Press, New York, 1959.
[27] E. Rozenthal, Y. Eckstein, Temperature gradients of subsurface of the Dead Sea area, Israel, Isr. J. Earth-Sci. 17 (1968) 131–136.
[28] Z. Ben-Avraham, R. Hanel, H. Villinger, Heat flow through the Dead Sea rift, Mar. Geol. 28 (1978) 253–267.
[29] Y. Eckstein, G. Simmons, Measurements and interpretation of terrestrial heat flow in Israel, Geothermics 6 (1978) 117–142.
[30] D. Levitte, A. Olshina, Isotherm and geothermal gradient maps of Israel, Geological Survey of Israel, Report GSI/60/84, Jarusalem, 1985.
[31] S. Feinstein, Constraints on the thermal history of the Dead Sea graben as revealed by coal ranks in deep bore holes, Tectonophysics 141 (1987) 135–150.
[32] S. Feinstein, B.R. Kohn, M. Eyal, Significance of combined vitrinite reflectance and fissiontrack studies in evaluating thermal history of sedimentary basin: an example from southern Israel, in: M.D. Noese, T.H. McCullah (Eds.), Thermal History of Sedimentary Basins: Methods and Case Histories, Springer—Verlag, Berlin, 1988, pp. 197–216.
[33] A. Bein, S. Feinstein, Late Cenozoic thermal gradients in Dead Sea transform system basins, J. Pet. Geol. 11 (1988) 185–192.
[34] B.P. Kohn, M. Eyal, S. Feinstein, A major Late Devonian–Early Carboniferous (Hercynian) thermotectonic event at the NW margin of the Arabian–Nubian Shield: evidence from zircon fission track dating, Tectonics 11 (5) (1992) 1018–1027.
[35] L.V. Eppelbaum, M.M. Modelevsky, A.N. Pilchin, Geothermal investigations in the Dead Sea Rift zone, Israel: implications for petroleum geology, J. Pet. Geol. 19 (4) (1996) 425–444.
[36] H. Gvirtzman, G. Garven, G. Gvirtzman, Thermal anomalies associated with forced and free ground-water convection in the Dead Sea rift valley, GSA Bull. 109 (9) (1997) 1167–1176.
[37] Z. Ben-Avraham, A. Ginzburg, J. Makris, L. Eppelbaum, Crustal structure of the Levant Basin, Eastern Mediterranean, Tectonophysics 346 (1–2) (2002) 23–43.
[38] V. Čermak, Crustal heat and mantle heat flow in Central and Eastern Europe, Tectonophysics 159 (1989) 195–215.
[39] A. Ginzburg, G. Gvirtzman, Changes in the crust and in the sedimentary cover across the transition from the Arabian platform to the Mediterranean basin: evidence from seismic refraction and sedimentary studies in Israel and in Sinai, Sediment. Geol. 23 (1979) 19–36.
[40] A. Ginzburg, J. Makris, K. Fuchs, B. Perathoner, C. Prodehl, Detailed structure of the crust and upper mantle along the Jordan–Dead Sea rift, J. Geophys. Res. 84 (B10) (1979) 5605–5612.
[41] J. Makris, Z. Ben-Avraham, A. Behre, A. Giese, L. Steinmetz, R.B. Whitmarsh, S. Eleftheriou, Seismic refraction profiles between Cyprus and Israel and their interpretation, Geophys. J. R. Astron. Soc. 75 (1983) 575–591.
[42] Z. Ben-Avraham, A. Ginzburg, Displaced terranes and crustal evolution of the Levant and the Eastern Mediterranean, Tectonics 9 (4) (1990) 613–622.
[43] L. Eppelbaum, A. Pilchin, New map of Moho discontinuity of Israel. Trans. of the Conf. of Israel Geol. Soc., Annual Meeting (1994) Ginossar, Israel, 23.
[44] A. Hofstetter, C. Dorbath, M. Rybakov, V. Goldshmidt, Crustal and upper mantle structure across the Dead Sea rift and Israel from teleseismic P-wave tomography and gravity data, Tectonophysics 327 (1–2) (2000) 37–59.
[45] K. Khair, G.N. Tsokas, T. Sawaf, Crustal structure of the northern Levant region: multiple source Werner deconvolution estimates for Bouguer gravity anomalies, Geophys. J. Int. 128 (1997) 605–616.
[46] Y. Folkman, A. Bein, Geophysical evidence for a pre-late Jurassic fossil continental margin oriented east–west under central Israel, Earth Planet. Sci. Lett. 39 (1978) 335–340.
[47] A. Ginzburg, Y. Folkman, The crustal structure between the Dead Sea Rift and the Mediterranean Sea, Earth Planet. Sci. Lett. 51 (1980) 181–188.
[48] J. Makris, C. Stobbe, Physical properties and state of the crust and upper mantle of the eastern Mediterranean Sea deduced from geophysical data, Mar. Geol. 55 (1984) 347–363.
[49] R. Bowenand, U. Jux, Afro-Arabian Geology, 1987, London–N.Y.
[50] Z. El-Isa, J. Mechie, C. Prodehl, J. Makris, R. Rihm, A crustal structure study of Jordan derived from seismic refraction data, Tectonophysics 138 (1987) 235–253.

[51] Z. El-Isa, Lithospheric structure of the Jordan–Dead Sea transform from earthquake data, Tectonophysics 180 (1990) 29–36.
[52] U. Ten Brink, N. Schoenberg, R. Kovach, Z. Ben-Avraham, Uplift and possible Moho offset across the Dead Sea transform, Tectonophysics 180 (1990) 71–85.
[53] A. Ginzburg, Y. Folkman, M. Rybakov, Y. Rotstein, Y. Assael, Z. Yuval, Israel: Bouguer Gravity Map, Scale 1:250,000 (1993), Survey of Israel.
[54] J. Makris, J. Wang, Bouguer gravity anomalies of the eastern Mediterranean Sea, in: V.A. Krasheninnikov, J.K. Hall (Eds.), Geological Structure of the Northeastern Mediterranean, 1994, pp. 87–98, Jerusalem.
[55] M. Rybakov, V. Goldshmidt, L. Fleisher, A new look at the Hebron magnetic anomaly, Isr. J. Earth-Sci. 44 (1995) 41–49.
[56] M. Rybakov, V. Goldshmidt, Y. Folkman, Y. Rotstein, Z. Ben Avraham, J. Hall, Magnetic map of Israel and adjacent areas (1:500,000), Inst. Petrol. Res. Geophys., (1994) Holon, Israel.
[57] M. Rybakov, V. Goldshmidt, Y. Rotstein, New compilation of the gravity and magnetic maps of the Levant, Geophys. Res. Lett. 24 (1997) 33–36.
[58] G.E. Brew, R.K. Litak, D. Seber, M. Barazangi, A. Al-Imam, T. Sawaf, Basement depth and sedimentary velocity structure in the northern Arabian platform, Eastern Syria, Geophys. J. Int. 128 (1997) 617–631.
[59] A.T. Batayneh, A.S. Al-Zoubi, The gravity field and crustal structure of the northwestern Arabian platform in Jordan, J. Afr. Earth Sci. 32 (1) (2001) 141–148.
[60] G.E. Brew, Tectonic evolution of Syria interpreted from integrated geophysical and geological analysis, Ph.D. Thesis (2001) Cornell University, Ithaca, NY, USA.
[61] A.N. Pilchin, L.V. Eppelbaum, Some peculiarities of thermodynamic conditions in the Earth's crust and upper mantle, Sci. Isr. 1–2 (2002) 117–142.
[62] V.G. Batanova, A.V. Sobolev, Compositional heterogeneity in subduction-related mantle peridotites, Troodos massif, Cyprus, Geology 28 (1) (2000) 55–58.
[63] A.H.F. Robertson, Overview of the genesis and emplacement of Mesozoic ophiolites in the Eastern Mediterranean Tethyan region, Lithos 65 (2002) 1–67.
[64] K.C. Condie, Plate Tectonics and Crustal Evolution, 4th ed. Butterworth Heinemann, Oxford, 1997.
[65] M. Beyth, The Precambrian magmatic rocks of Timna valley, Southern Israel, Precambrian Res. 36 (1987) 21–38.
[66] M. Beyth, F.J. Longstaffe, A. Ayalon, A. Matthews, Epigenetic alteration of the Precambrian igneous complex at Mount Timna, southern Israel: oxygen-isotope studies, Isr. J. Earth-Sci. 46 (1997) 1–11.
[67] M. Beyth, T. Reischmann, The age of the quartz monzodiorite, the youngest plutonic intrusion in the Timna Igneous Complex, Isr. J. Earth-Sci. 45 (1996) 223–226.
[68] G. Baer, A. Heimann, Y. Eshet, R. Weinberger, A. Musset, G. Sherwood, The Saharonim Basalt: a late triassic–early Jurassic intrusion in southeastern Makhtesh Ramon, Israel, Isr. J. Earth-Sci. 44 (1995) 1–10.
[69] N. Teutsch, A. Ayalon, Y. Kolodny, Late Cretaceous exposure and paleoweathering of a basaltic dike, Makhtesh Ramon, Israel: geochemical and stable isotope studies, Isr. J. Earth-Sci. 45 (1996) 19–30.
[70] B.P. Kohn, B. Lang, G. Steinitz, $^{40}Ar/^{39}Ar$ of the Atlit-1 volcanic sequence, northern Israel, Isr. J. Earth-Sci. 42 (1993) 17–28.
[71] S. Feinstein, Vitrinite reflectance and maximum heating of the Lower Jurassic Inmar Formation in Southern Israel, Isr. J. Earth-Sci. 45 (1996) 1–10.
[72] A. Polat, J.F. Casey, R. Kerrich, Geochemical characteristics of accreted material beneath the Pozanti–Karsanti ophiolite, Turkey: intra-oceanic detachment, assembly and obduction, Tectonophysics 263 (1996) 249–276.
[73] L.V. Eppelbaum, S.V. Kouznetsov, V.L. Vaksman, C.A. Klepatch, S.A. Smirnov, L.M. Sazonova, N.N. Korotaeva, A.V. Surkov, S.E. Itkis, M. Shemesh, Results of integrated geological–geophysical examination of Makhtesh Ramon area (southern Israel) on diamond-bearing associations, Coll. of Selected Papers of the SPIE Conference, Section: Geology and Remote Sensing, 2003, pp. 109–120, Barcelona, Spain.
[74] S.E. Haggerty, M.S. Nagieb, Diamonds in non-kimberlitic, non-lamproitic diatremes from Northwest Syria, Trans. of 28th Internat. Geol. Congress, vol. 2, 1989, pp. 2.6–2.7.
[75] Ye.V. Sharkov, Ye.Ye. Laz'ko, S. Hanna, Plutonic xenoliths from the Nabi Matta explosive center, Northwest Syria, Geochem. Int. 30 (4) (1993) 23–44.
[76] P. Morgan, Diamond exploration from the bottom up: regional geophysical signatures of lithosphere conditions favorable for diamond exploration, J. Geochem. Explor. 53 (1995) 145–165.
[77] S. Ballard, H.N. Pollack, Diversion of heat by Archean cratons, Earth Planet. Sci. Lett. 85 (1987) 253–264.
[78] A.E. Shimron, The Dahab mafic–ultramafic complex, southern Sinai Peninsula—a probable ophiolite of Late Proterozoic (–Pan African) age, Ofioliti 6 (1) (1981) 161–164.
[79] B.B.M. De Lawrence, Curie surface of the central Goiás region and relationships with geology, geotectonics and mineral resources, MSc Thesis (1995) No. 96, University of Brasilia—Institute of Geosciences.
[80] R. Pucher, Pyrrhotite-induced aeromagnetic anomalies in western Germany, J. Appl. Geophys. 32 (1994) 33–42.
[81] R. Pucher, T. Wonik, A new interpretation of the MAGSAT anomalies of Central Europe, Phys. Chem. Earth 23 (9–10) (1998) 981–985.
[82] J.M. Kovalik, J.L. Kirschvink, New superconducting-quantum-interference-device-based constraints on the abundance of magnetic monopoles trapped in matter: an investigation of deeply buried rocks, Phys. Rev. 33 (2) (1986) 1184–1187.
[83] L. Eppelbaum, Z. Ben-Avraham, Hebron magnetic anomaly: integrated analysis of potential geophysical fields, Rep. for the Ministry of Infrastructure and Energy of Israel, 2002, ES-24-02.
[84] L. Eppelbaum, Z. Ben-Avraham, Y. Katz, Does mantle diapir produce Hebron magnetic anomaly? Trans. of the Conf. of the Israel Geol. Soc. Ann. Meet., Moshabim Country Logging (Negev), Israel, 2005, p. 26.
[85] D.D. Blackwell, The thermal structure of the continental crust, in: J.D. Heacock (Ed.), The Structure and Physical Properties of the Earth's Crust, AGU, Geophys. Monogr. Ser., vol. 14, 1971, pp. 169–184.
[86] M. Nathenson, M. Guffanti, Geothermal gradients in the Conterminous United States, J. Geophys. Res. 93 (B6) (1988) 6437–6450.
[87] B.K. Bhattacharyya, L.W. Morley, The delineation of deep crustal magnetic bodies from total field aeromagnetic anomalies, J. Geomagn. Geoelectr. 17 (1965) 237–252.
[88] R.T. Shuey, D.K. Schellinger, A.C. Tripp, L.B. Alley, Curie depth determination from aeromagnetic spectra, Geophys. J. R. Astron. Soc. 50 (1977) 75–101.

[89] A. Salem, K. Ushijima, A. Elsirafi, H. Mizunaga, Spectral analysis of aeromagnetic data for geothermal reconnaissance of Quseir area, Northern Red Sea, Egypt, Proc. of the World Geothermal Congress (2000) Kyushu-Tohoku, Japan, 2000, pp. 1669–1674.
[90] Y. Okubo, R.J. Graf, R.O. Hansent, K. Ogawa, H. Tsu, Curie point depths of the island of Kyushu and surrounding areas Japan, Geophysics 53 (1985) 481–494.
[91] R.J. Blakely, Curie temperature isotherm analysis and tectonic implications of aeromagnetic data from Nevada, J. Geophys. Res. 93 (1988) 817–832.
[92] G. Connard, R. Couch, M. Gemperle, Analysis of aeromagnetic measurements from the Cascade Range in central Oregon, Geophysics 48 (1983) 376–390.
[93] W.G. Powell, D.S. Chapman, A detailed study of heat flow at the Fifth Water site, Utah, in the Basin and Range—Colorado Plateaus transition, Tectonophysics 176 (1990) 291–314.
[94] J.H. Sass, S.S. Priest, L.E. Duda, C.C. Carson, J.D. Hendricks, L.C. Robinson, Thermal regime of the State 2–14 Well, Salton Sea scientific drilling project, J. Geophys. Res. 93 (B11) (1988) 12995–13004.
[95] R.F. De Rito, A.H. Lachenbruch, T.H. Moses Jr., R.J. Munroe, Heat flow and thermotectonic problems of the Central Ventura basin, Southern California, J. Geophys. Res. 94 (B1) (1989) 681–699.
[96] J.A. Majorowicz, F.W. Jones, A.M. Jessop, Geothermics of the Williston basin in Canada in relation to hydrodynamics and hydrocarbon occurrences, Geophysics 51 (3) (1986) 767–779.
[97] M.A. Speece, T.D. Bowen, J.L. Folcik, H.N. Pollack, Analysis of temperatures in sedimentary basins: the Michigan Basin, Geophysics 50 (8) (1985) 1318–1334.